Methanol Production from Excess Electricity

Dennis Espert, Kaspar Eucken, Kevin Emmanuel Lienou Ngomsu,
Hardik Mhatre, Maik-Alexander Sauck
Hamburg University of Technology

Contents

1 Introduction

Due to climate change and as a contribution to the goals of the Paris agreement, the chemical industry has to move to renewable energy and reduce their CO_2 emissions. For this work, a new chemical process with the use of CO_2 and renewable energy in Belgium has to be developed. The aim is to design a sustainable methanol production process that integrates captured CO_2 and green H_2 and by that contributes to the successful energy transition and grid stability. Methanol as a product was chosen since it does not only have a wide range of applications but is also seen as a possible candidate to play a key role in a defossilized economy [1]. Also, the production process of "green" Methanol is an existing concept in science, and partly implemented in industry [2], yet a lot of challenges remain until higher market penetration - allowing us to develop our own process with meaningful improvements and optimizations.

H_2 is produced by a electrolyser plant, stored in a buffer tank and then fed into the methanol production process. In the process, as much H_2 as possible is recycled due to the fact, that H_2 is the limiting component in the process. The process is designed to integrate most of the heat by heat exchangers or by upgrading the low quality heat for the production of low pressure stream or for district heating.

2 Overall Concept

2.1 Location Assessment

The port of Antwerp in Belgium was chosen since it has some great advantages and offers a good flexibility in planning. First, a large variety of industries are localized there, including chemical plants with a huge demand for methanol, e.g BASF. At the same time the port of Antwerp together with Air Liquide and the EU are actively involved in projects like Antwerp@C [3] which is a centralized CO_2 storage unit in the harbor and provides a great carbon source. The proximity to the infrastructure of the port also offers short ways to potential markets e.g. export or green ship methanol [4].

2.2 Methanol reaction

The hydrogenation of CO_2 to methanol is done directly (Eq. 1) or indirectly with the Reverse Water Gas Shift (RWGS, Eq. 3) reaction forming CO which then reacts with H_2 to methanol (Eq. 2). All three reactions occur in parallel. Reaction 1 and 2 are exothermic whereas 3 is endothermic [5].

$$CO_2 + 3\,H_2 \rightleftharpoons CH_3OH + H_2O, \quad \Delta H_R = -87 \text{ kJ/mol (298 K)} \tag{1}$$

$$CO + 2\,H_2 \rightleftharpoons CH_3OH, \quad \Delta H_R = -128 \text{ kJ/mol (298 K)} \tag{2}$$

$$CO_2 + H_2 \rightleftharpoons CO + H_2O, \quad \Delta H_R = +41 \text{ kJ/mol (298 K)} \tag{3}$$

2.3 Discontinous operation

To reduce electricity costs and profit from "surplus-electricity" in volatile markets [6] the discontinous operability of the process was taken into account. An upper limit price of 50 €/MWh was chosen for H_2 production. Using an electrolyzer capacity of 100 MW, producing 1875 kg/h [7], this results in electricity costs for H_2 less than 2.67 €/kg. Similar price ranges are reported for the production cost of green H_2 [8, 9]. To decouple electrolysis and methanol production a buffer tank capacity of 50 tonnes was chosen.

3 Process Modeling

3.1 Continous Process

The overall continuous process is modeled with Aspen Plus. The substances Hydrogen (H_2), carbonmonoxid (CO), carbondioxid (CO_2), methanol (CH_3OH) and water (H_2O) occur in the process. Due to the high pressure in the reactor, Soave-Redlich-Kwong (RK-SOave) is used as property method for the thermodynamic model [10]. The process can be seen in Figure 1.

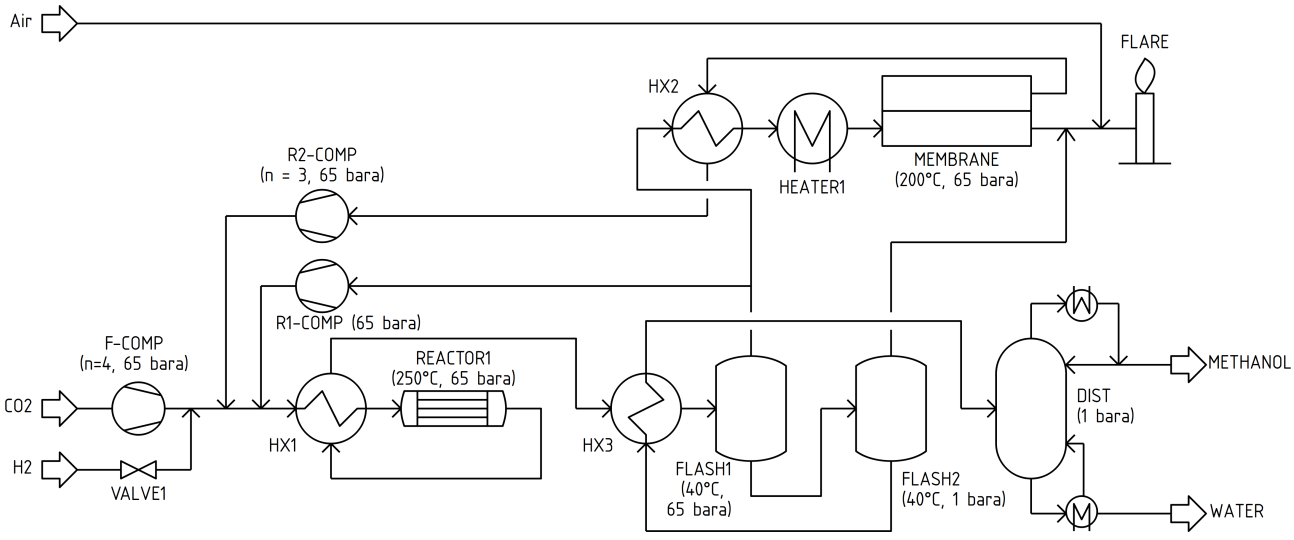

Figure 1: Flowsheet of continous process

The process has two feed streams. The first one (CO2) is a CO_2 stream and compressed to 65 bar. The second one (H2) is a stream with dry H_2 at high pressure, which is lowered to 65 bar.. The CO_2 stream is chosen for a ratio of H_2 to CO_2 of 3 in the inlet stream of the reactor. After mixing the two feed streams and two recycle streams (RECYCLE1, RECYCLE2), the stream REAC-MIX is preheated to 240°C and fed into the reactor (REACTOR1).

After the reactor, the output stream is used in a heat exchanger (HX1) to preheat the reactor inlet stream and in another heat exchanger (HX3) to preheat the feed stream for the distillation column (DIST). After that product stream is flashed two times (FLASH1, FLASH2). The vapor stream of FLASH2 is purged, while the liquid stream is fed into the distillation column (DIST) after preheating to 71°C.

The vapor stream of the first flash unit (FLASH1) is split into two recycle streams (RECYCLE1, RECYCLE2) with a split ratio of 0.15, which was found to be optimal for minimal hydrogen loss and maximum carbon dioxide recovery, as shown in Table A.11, which are later mixed into the reactor feed stream to recyvle unconverted H_2 and CO_2. RECYCLE1 needs a pressure increase (R1-COMP) to compensate pressure losses. RECYCLE2 is first heated with a heat exchanger (HX2) and an auxiliary heater (HEATER1) to 200°C for a membrane (MEMBRANE) to recover H_2 and some CO and CO_2 in the permeate. The permeate stream has to be compressed to 65 bars (R2-COMP) because of the pressure drop in the membrane.

The pressure increase in the streams is made by multistage compressors (F-COMP, R2-COMP) with interstage cooling to 50°C and an isentropic efficiency of 0.85 and mechanic efficiency of 0.95. The last compressor of F-COMP and R2-COMP compresses the stream with a different compression ratio than the compressors before to the required pressure of 65 bar and a temperature of around 150°C, which is used as an upper temperature limit for compressors. With that, the increase in temperature while compression of gases can be used to reduce the amount of heat duty in the upcoming feed preheating.

For heat integration, three heat exchangers are incorporated with countercurrent flow and a minimum temperature difference between the hot and cold streams of 10 K. Two heat exchangers (HX1, HX3) use the hot temperatures in the reactor and therefore the product stream from the reactor (REACTOR1). In those heat exchangers the hot stream is used to preheat the reaction and distillation inlet streams, so there is no additional heating required. In heat exchanger HX2 the permeate is used for preheating the membrane feed, which has to be heated for the membrane, and is cooled down to 50°C which is required for the multistage compressor. Here, an additional heater must be used for the membrane feed, but the heat demand can be decreased by 81%. When using cooling water, the minimum temperature that can be achieved for the cooled stream is 40°C [11]. Because of this, the temperatures in the interstage cooling and during the flashes are 50°C respectively 40°C.

3.2 Reactor Model

The catalytic reaction in the equations 1, 2 and 3 with a fibrious Cu/Zn/Al/Zr catalyst are described with Langmuir-Hinshelwood-Hougen-Watson (LHHW) kinetics. The kinetic factors as well as factors for the driving forces and adsorption are required in Aspen Plus for all three reactions and can be found in the work of Kiss et al. [10].

An isothermic RPlug model with 420 tubes and 450 kg catalyst was chosen for the reactor. The reaction conditions are 250°C and 65 bar. A multitube reactor increases the cooling surface and allows better control of the reaction temperature. The reactor is 12 m long and each tube has a diameter of 0.06 m, the bed voidage of the catalyst is 0.98. The dimensions and catalyst bed were chosen on the basis of Kiss et al. [10]. A reactor yield of 0.25 was achieved, which is slightly higher than achieved by Kiss et al. [10], with 0.11 to 0.16 in a temperature range from 210°C to 270°C.

3.3 Methanol separation

The separation of methanol takes place in the distillation column. However, before this step, the gaseous components (H_2, CO, and CO_2) are separated from the liquid phase in two flash units.

Flash 1: Initial Separation of Gases In the first flash unit (FLASH1), the gaseous components are separated from the liquid phase which consists of methanol, water and dissolved gases. A temperature of 40°C and a pressure of 65 bar were set. This pressure corresponds to the reaction pressure. The heat dissipated in this process step is 2307.41 kW. The temperature of 40°C was chosen because methanol and water remain in the liquid phase at this temperature due to higher boiling points. Lowering the temperature improves the condensation of the liquids, while the gases remain in the vapor phase [10]. After separation, the molecular fractions of methanol and water in the liquid phase are 0.486 and 0.494 respectively.

Flash 2: Removal of dissolved gases In the second flash unit (FLASH2), the remaining dissolved gases are removed from the liquid. The pressure is lowered to 1.013 bar, while the temperature is kept constant at 40°C. The phase is again vapor-liquid. The heat supplied in this process step is 6.076 kW. By lowering the pressure, the gases dissolved in the liquid return to the vapor phase. This happens because the solubility of gases decreases with decreasing pressure [10]. After this second separation, the molecular fractions of methanol and water in the liquid phase are 0.494 and 0.505 respectively, which shows that the liquid has been almost completely freed of gases.

Distillation Once the gaseous components have been separated, distillation takes place in a distillation column to further purify the methanol. By analyzing the Tx diagram at 1 atm, it can be determined that no azeotrope exists between methanol and water. The selected method to describe the phase equilibrium is the RK-Soave model. This method offers advantages such as a more accurate description of the phase behavior in systems with non-ideal gases. Since there is a very small amount of gases, less than 1%, in the feed, this method was used for better modeling of the separation [10]. First, the DSTWU shortcut model was used to design the rectification column. In order to achieve the required methanol purity, the following parameters were determined in the Table 1:

Table 1: Calculated values using the DSTWU model

Parameter	**Value [-]**
Minimum Reflux Ratio	0.376
Actual Reflux Ratio	0.404
Minimum number of stages	5
Number of actual stages	30

These values were rounded up and multiplied by a safety factor of 1.5 to obtain an initial estimate for the more precise RadFrac model (DIST). The separation of methanol was initially calculated with a number of stages of 45 and a reflux ratio of 0.6. A distillate rate of 100 kmol/h was implemented as this corresponds to the amount of methanol in the feed stream to be withdrawn at the top of the column. In addition, with a sensitivity analysis the required number of stages in the column are determined with 47 for a methanol purity of 0.995. Further sensitivity analyses were carried out to determine optimum values for the reflux ratio 0.7 and for the feed stage 39. The energy input required for the distillation in the reboiler is 1845.246 kW. In the condenser, 1865.23 kW must be dissipated in order to condense the vapor streams.

3.4 Membrane Separation

To prevent methanol and water buildup, a portion of the FLASH1 vapor stream is purged. The simulation results show that the purge stream contains significant H_2. Its recovery is crucial, as it is one of the most expensive reactants in the production costs of green methanol [12]. Various methods, including pressure swing adsorption and membrane separation, can recover H_2. Membrane separation is widely used in industries such as hydrocarbon refining and ammonia production [13, 14]. For the

CO_2 hydrogenation reactor, high H_2 selectivity is less critical, as the purge stream mainly contains CO_2, CO, methanol, and water in minor amounts. CO in the purge stream surpresses the RWGS reaction and aids methanol formation [15]. Hence, a polymeric membrane was chosen due to its low cost and the goal of maximizing H_2 recovery [13].

A Python-based mathematical model was developed to evaluate the membrane's performance. The simulation was conducted under the assumption of steady-state operation. The membrane was discretized along its length to iteratively solve the transport equations for all components. At each discretized step, the retentate and permeate streams were assumed to be well-mixed. To account for non-ideal gas behavior dute to a pressure of 65 bar, the compressibility factor (Z) for each component was determined using the Peng-Robinson equation of state. Additionally, no chemical reactions were assumed to occur within the membrane module, and the pressure drop on the permeate side was considered constant. The temperature was also assumed to remain uniform across the membrane. This approach has been validated in literature [16]. Initially, the membrane is solved to determine the composition of the permeate and retentate streams. As this is a multicomponent system, the permeability of each component across the membrane depends on the feed composition and temperature. However, permeability remains nearly constant at a fixed temperature and does not vary significantly with pressure [17]. Therefore, the mole fraction of each component is used to calculate its permeability.

The variation in permeability with feed composition can complicate the calculation of flux. To handle this, the permeability values, the partial pressure and fugacity of each component is updated in each iteration. The fugacity difference across the membrane, which serves as the driving force for permeation, is used to calculate the permeation rate and the permeate flow rate. The individual component flow rates in both the permeate and retentate streams are summed to calculate the total flow rates at the membrane outlet. The feed data from the Aspen simulation was used to simulate the membrane module separately. Its composition, temperature, and pressure were input into the Python simulation, and the resulting split fractions for the permeate stream were then fed into the Aspen Plus separator (SEP) model. This approach allowed for an approximate replication of the stream composition. To validate the simulation, the membrane was tested with varying feed compositions, revealing that the split fraction remained relatively stable. The simulation was then used to optimize the membrane area and stage cut to minimize H_2 loss. For the Aspen Plus-simulated feed, a membrane area of 103 m^2 and a stage cut of 0.9 resulted in a H_2 loss of approximately 1.85 mol%, as illustrated in Figure 2a.

A comparative study evaluated the process with and without a membrane based on mol% CO_2 utilized, mol% H_2 utilized, mol% CO_2 loss, mol% H_2 loss and carbon yield to methanol. Incorporating the membrane significantly reduced hydrogen loss, improving H_2 utilization, while CO_2 utilization also increased, although to a lesser extent. The CO concentration in the purge stream decreased as more CO was converted to methanol, but the carbon yield to methanol decreased to 88%. These results are summarized in Figure 2b.

3.5 Discontinous Behaviour

Since it is part of the concept to operate at times where the electricity price is in a feasible range, the trend of spotmarket electricity prices for 2024 in Belgium was investigated [18]. To investigate the non-continous operability of the process under economic aspects, the accumulation of hydrogen $m_{H_2}(t)$ in a buffer tank was modeled using equations 4 and 5.

$$\frac{dm_{H_2}}{dt} = capacity \cdot production_{H_2} \cdot mode(t) - demand_{H_2} \tag{4}$$

$$m_{H_2}(t) = capacity \cdot production_{H_2} \cdot \int mode(t)\, dt - demand_{H_2} \cdot t \tag{5}$$

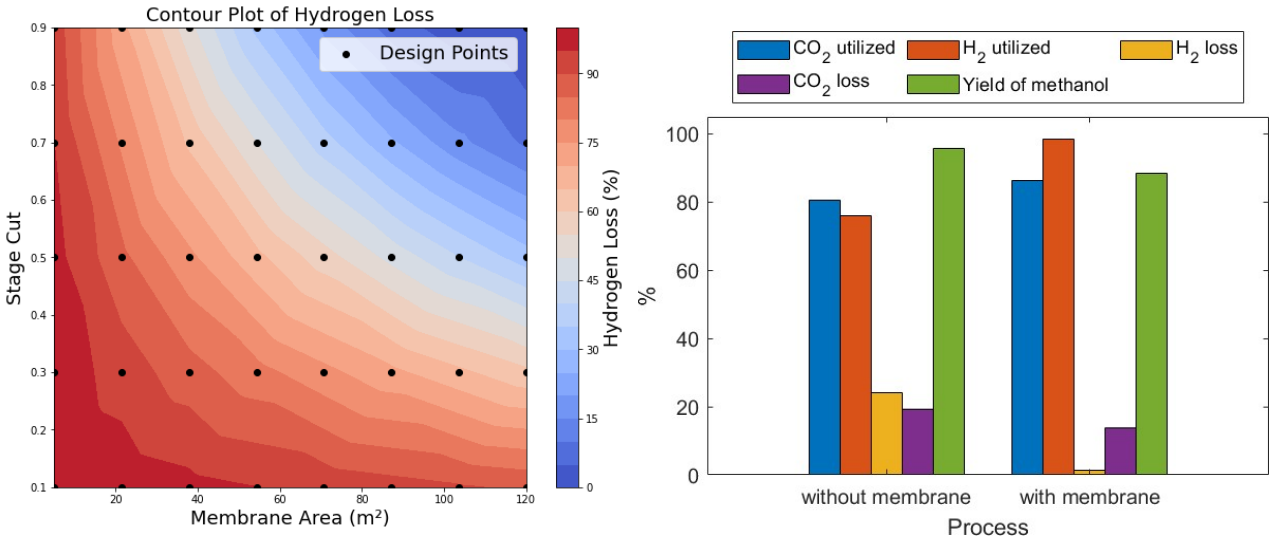

(a) Contour for membrane area and stage cut against % Hydrogen Loss

(b) Comparing process with and without membrane

Figure 2: Membrane results

The overall methanol production capacity was assumed to be 20,000 t/year which leads to a continous hydrogen demand of 635 kg/h assuming an operating time of 8,000 h/year. Electrolyzer capacity is assumed to be 100 MW. $production_{H_2}$ is 18.75 kg/h, assuming a production rate of 450 kg_{H_2}per 1 MW electrolyzer module as stated by QuestOne [7]. The marginal prices are assumed to be 50 €, 40 € and 30 € to show how the variation of the marginal price influences the operation behaviour. A hydrogen tank capacity of 50,000 kg was chosen. Applying the conversion factor of 14.5 kg/m^3 as given by Klingler et al. [19] gives a tank volume slightly more than 3000 m^3. Under similar conditions also a H_2 storage capacity of 200 tons to 1000 tons resulted using optimization approaches [20].

To achieve economic feasibility the downtime and the amount of start-ups and shut-downs of the plant must be reduced. In Table 2 the overall downtime of the plant and the amount of downtimes for the year 2024 for six different scenarios is displayed. The marginal price is varied from 30, 40 and 50 €/MW. The results for 30 and 50 €/MW are displayed in Figure 3. The downtime and the amount of downtimes are also displayed for a scenario where no H_2 is available, to show the effect of the buffer tank. Even when not clearly visible in Figure 3, it is proved in Table 2 that the installation of a 50 tons H_2-storage significantly reduces the overall downtime and the amount of downtimes for the methanol plant in flexible operation.

Table 2: Shut down time and amount of start-up and shut-down processes

Marginal price [€/MWh]	**H_2 storage [t]**	**Downtime [h]**	**Amount of downtimes**
50	50	2861	82
40	50	3965	97
30	50	4837	96
50	0	6442	325
40	0	7006	250
30	0	7380	202

Influence of non-continuous behavior on OPEX and revenue

In the downtime of the methanol plant no product is produced, and also it is assumed that no energy costs are caused. The amount of downtimes has an effect on the operational costs in that sense, that

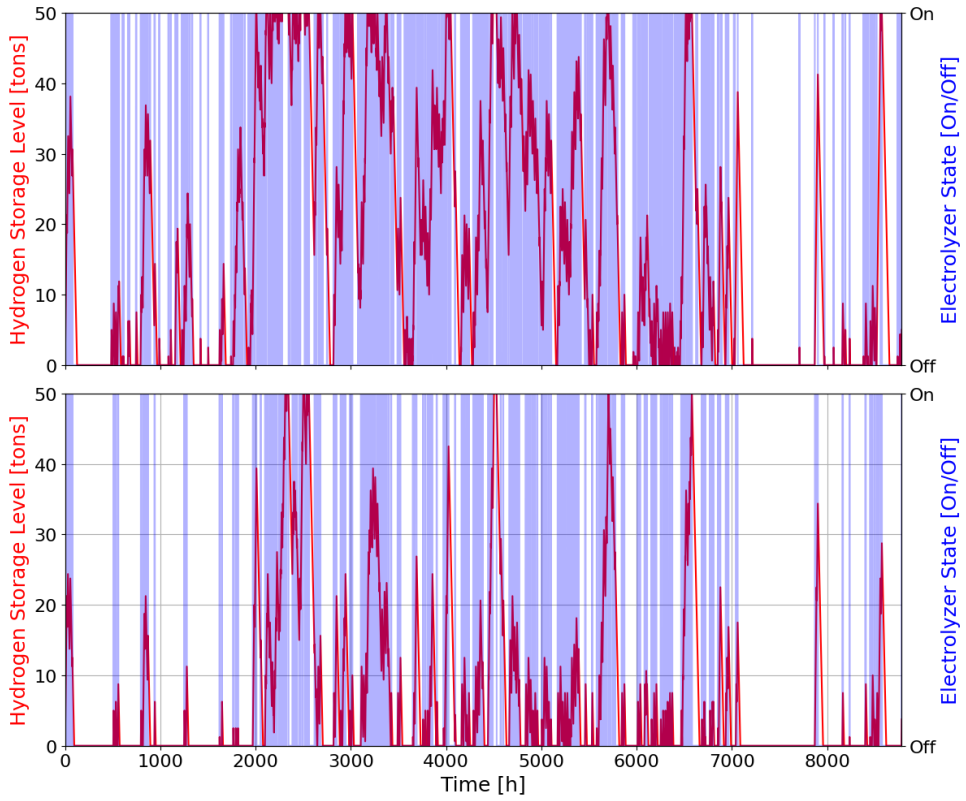

Figure 3: Hydrogen accumulation and operation mode at a marginal price of 30 €/MWh (top) and 50 €/MWh (bottom)

energy costs are generated for a start-up and a shut-down process. There will be product generated, but it is not clear whether the product fulfils the specifications and can be sold for profit. To include the effect of start-up and shut-down on the costs, two extreme scenarios are considered. For both scenarios, a ramp rate of 50% load/h will be considered, which is found to be the less optimal case resulting from studies [21, 22]. This results in a start-up/shut-down time of four hours in total for every downtime.

In the best case, for four hours 50% of possible valuable product is produced, while 50% of energy costs are generated. It is based on the assumption that the inputs an outputs directly depend on the load of the methanol plant. In the worst case, for four hours no valuable product is produced, while 150% of energy costs are generated. It is is based on the assumption that a higher amount of energy is required while the start-up/shut down process. The numbers are assumed since the start-up/shut-down process of a methanol plant was barely investigated in literature. Research on the start-up/shut-down process of methanol synthesis reactors was carried out by Ash-Kurlander et al. [23], Gao et al. [24] and Matthischke et al. [25]. The evaluation of both scenarios will be further considered in the cost analysis.

3.6 Energy-integrated distillation

The distillation column (DIST) in the Aspen Plus simulation is not heat-integrated, but with different energy integration methods, the energy demand of the separation can be reduced. For the evaluation of different integrated distillation columns, the tool presented in Skiborowski [26] is used. This tool calculates the minimum energy demand (MED) on the base of the rectification body method [27] and the operating and investment costs of various distillation processes. The screening tool applies energy integration methods such as multi-effect distillation or vapor recompression (VRC) and was further

developed for the use of closed-cycle heat pumps (EHP) with various refrigerants. With this tool, a qualitative statement about energy and cost reduction can be made. The feed mole flow as well as the feed and product compositions and the column pressure are taken from the Aspen Plus simulation. As a simplification, the presence of hydrogen and carbon monoxide is neglected. The thermodynamic models are NRTL as g^E model and Redlich-Kwong as EOS model. A simple column and its VRC and EHP process alternatives are calculated.

With an upper bound for the compressor outlet temperature of 150°C and a compression ratio of 7, 26 process alternatives are evaluated. The energy demand of the column in the Aspen Plus simulation is in the same range as the simple column without any integration in the screening tool simulation, which validates the results. The difference can be explained with the different models since Aspen Plus is using a rigorous calculation with a finite number of equilibrium stages whereas the screening tool calculates the lower bound of the energy demand with an infinite number of stages and the presence of trace elements in the feed stream of the Aspen Plus simulation. The minimum energy demand of the base column (BASE) and the columns with the best three refrigerants for closed cycle heat pumps (EHP) are shown on the left in Figure 4.

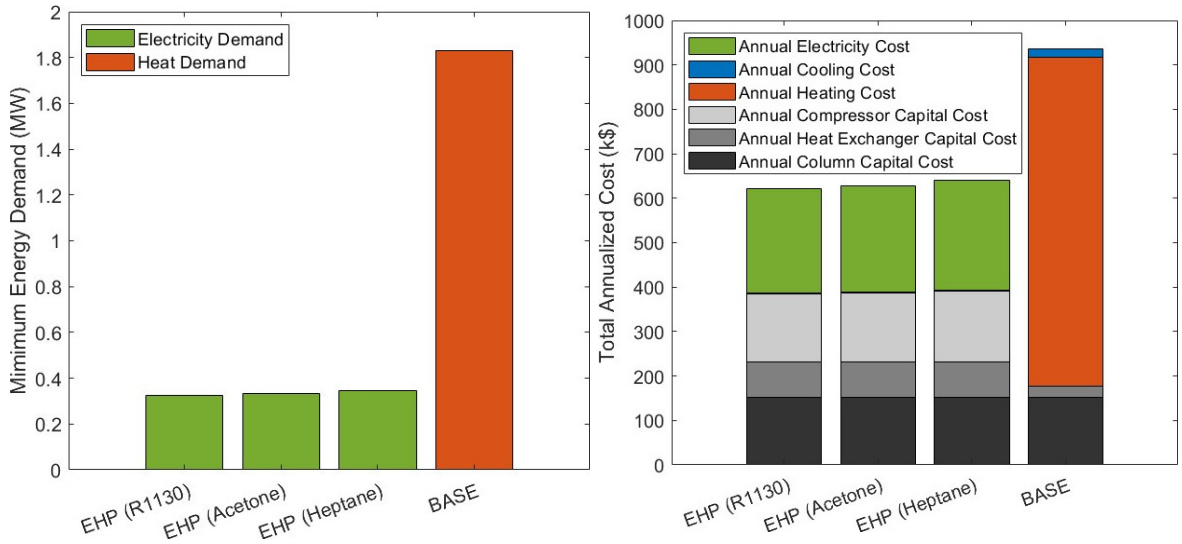

Figure 4: Minimum energy demand (left) and annualized total costs (right) of the distillation

The MED of the distillation process can be reduced by using a closed cycle heat pump by up to 82% depending on the refrigerant. The EHP alternatives are also fully electrified. A simple column with EHP and R1130 as refrigerant has the lowest energy demand with 0.327 MW in comparison to the base column (BASE) with a energy demand of 1.832 MW. Because of an Ozone Depletion Potential greater than zero of R1130 [28], the use of an organic refrigerant such as acetone as the second best and heptane as the third best result should be considered, which still reduces the Energy demand by over 80%. Other criteria for feasible refrigerants are the Global Warming Potential, the toxicity and the flammability of the refrigerants. The annualized investment and operating costs with a depreciation period of 10 years are shown on the right in Figure 4. The case study demonstrates that a column equipped with an external heat pump can reduce the operation cost by 69% and the annualized total cost by 34%. The lower cost reduction in the annualized total cost in comparison to the operation cost results from additional heat exchangers and compressors which are required in the closed cycle heat pump.

3.7 Waste Heat Recovery

The process considered here is generating a significant amount of heat [5]. Much of this heat is of low quality, leading to substantial exergy losses [12]. To maximize heat recovery and enhance its usability,

various techniques were implemented to convert this low-quality heat into a more useful form.

To convert low-grade heat into useful form, industry typically uses waste heat from processes to generate hot water for district heating [29]. The Organic Rankine Cycle (ORC) is also commonly employed, converting low to medium-grade heat with generating steam into electricity [30, 12]. As the steam and source temperatures are not very high, the amount of energy generated from this method is limited. Other methods, such as the Kalina cycle and the trilateral cycle, can also be used for heat recovery [29].

Our calculations show that most of the heat comes from FLASH1 (31.60%), followed by DIST (25.60%) and REACTOR1 (28.7%). The REACTOR1 operates at 250°C, while FLASH1 operates at 118°C, generating medium-grade heat. To reduce exergy destruction, the cooling water is preheated in multiple steps before being supplied to the reactor at temperatures close to its operating temperature. The steam produced is used to generate power while lowering the steam pressure[12]. After electricity generation, low-pressure steam (10 bar, 180°C) can be sold to industry or a carbon capture plant. The hot water from the steam process and earlier steps, at various temperatures, is used to generate electricity via ORC. The cooled water from the ORC process (79–80°C) can then be used for district heating. The flowsheet for the heat recovery simulation is shown in Figure A.4.

The working fluids for the ORC were compared based on their net power output , thermal efficiency, and exergy efficiency. R11 yielded a net power output of 105.38 kW, with a thermal efficiency of 30.94% and an exergy efficiency of 52.15%. Pentane produced 86.87 kW of net power, achieving thermal and exergy efficiencies of 30.94% and 43.97%, respectively. Hexane generated 103.81 kW, with thermal and exergy efficiencies of 31.13% and 50.44%. Butane resulted in 101.65 kW of net power, with thermal and exergy efficiencies of 30.57% and 52.51%, respectively. From those working fluids pentane was chosen due to its beneficial properties as a ORC working fluid [31].

4 Cost Analysis

4.1 CAPEX

The Capital Expenditures, or 'CapEx', refers to a company's investments in long-term assets such as buildings, land, machinery or equipment. This expenditure is used to acquire, improve or maintain these assets and contributes to the company's long-term value creation [32].

Cost curves for acquisition costs of plant equipment

Correlations in Table A.2 are used as a first approximation for cost estimates. The general form of the correlations used is shown in equation 6:

$$C_e = a + b \cdot S^n \tag{6}$$

where: C_e is purchased equipment cost on a U.S. Gulf Coast basis (2010), a and b are cost constants, S is the size parameter, n is an exponent for that type of equipment. Table A.2 shows the calculated acquisition costs for the plant equipment used in tabular form [33].

Material factors

If the acquisition costs were calculated on a special alloy basis, the other installation factors must be adjusted accordingly to avoid overestimating the installation costs. The total installation costs can be calculated using equation 7.

$$C = \sum_{i=1}^{M} C_{e,i,A} \left[(1 + f_p) + \frac{(f_{er} + f_{el} + f_i + f_c + f_s + f_l)}{f_m} \right] \tag{7}$$

where $C_{e,i,A}$ is the purchased cost of equipment in alloy, and M is the total number of equipment. The specific values of the installation factors are listed in Table A.3. The values f_i are the installation factors, in which f_p stands for the piping, f_{er} for the equipment erection, f_{el} for the electrical work, f_i for instrumentation and process control, f_c for civil engineering, f_s for structures and buildings, f_l for lagging, insulation and paint and f_m for the steel relative to plain carbon steel [33].

Cost escalation

A frequently used method for updating historical costs is the use of published cost indices which set current costs in relation to previous costs and are based on statistical surveys of labor, material and energy costs. The cost adjustment can be calculated using equation 8 [33].

$$\text{Cost in year A} = \text{Cost in year B} \cdot \frac{\text{Cost index in year A}}{\text{Cost index in year B}} \tag{8}$$

The cost index in 2010 and 2025 is 550.8 and 798.8 respectively [34].

Investment costs

The investment costs of the methanol plant amount to 22,449,337.2 €. They are calculated and tabulated in Table A.4. Costs were converted into euros based on an exchange rate of 1USD = 0.9556 €[35]. The specific costs for an H_2 tank are 45 €/Nm^3. A factor of 1 Nm^3 = 0.08988 kg is used to convert the gas volume [36]. As a tank with a capacity of 50 tons is required, the investment costs for the tank amounts to 25,033,377.84 €.

To determine the investment costs of the electrolyser the specific costs per kilowatt were calculated. These relate to the total installed capacity of the electrolyser. The total costs are made up of various components, whereby the costs for the stack are 309.48 €/kW, for the Mechanical Balance of Plant (MBoP) 123.49 €/kW and for the Electrical Balance of Plant (EBoP) 109.49 €/kW. This results in a total investment of 542.04 €/kW for the electrolyser. The MBoP comprises various components that are required for electrolyser operation such as pumps, heat exchangers, water treatment systems, gas separators, pipework and the structural support of the plant. The EBoP includes all electrical components required for the power supply and control of the electrolyser. This includes power electronics, transformers, rectifiers, inverters, sensors, control systems and plant cabling [36, 37]. 80 stacks are required resulting in a capacity of 100 MW. The investment costs for the electrolyser amount to 54,204,000 €. The total investment costs amount to 101,686,715 €. The proportions of the investment costs are shown in Figure 5 (left).

4.2 OPEX

The operational expenditures (OPEX) were calculated per year with the usage of data from literature. The highest variable cost is the cost for electricity. This is a variable cost and was connected to the dynamic electricity price discussed in chapter "Dynamic Behaviour". The plant is separated into two parts, which are not always operating at the same time. The electrolysis section for producing the hydrogen and the methanol plant. Both plants have distinct yearly operational hours and different resulting average electricity prices. The electrolysis part of the plant is expected to run 2342 h/year (see chapter 3.5) and following from that, the methanol part is expected to run 5899 h/year. The variable cost, e.g. electricity, water, catalyst, and CO_2 are presented in Table 3.

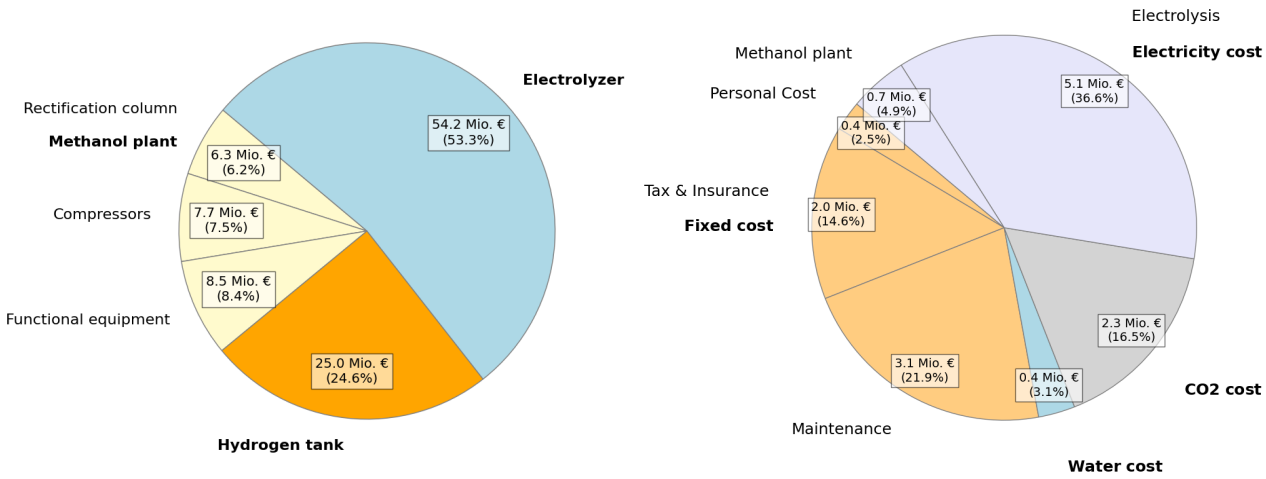

Figure 5: Proportions of CAPEX (left) and OPEX (right)

Table 3: Variable operating cost

Cost Item	Specific Cost	Variable Cost	Reference Source
Electricity Electrolysis	0.02178 €/kWh	5,100,876 €	[18]
Electricity Methanol	0.04489 €/kWh	700,230 €	[18]
Water	0.01 €/kg	430,928 €	[38]
CO_2	0,08 €/kg;	2,294,873 €	[39]
Catalyst	18.1 €/kg	2,444 €	[40]

The CO_2 cost, as explained in the chapter "Carbon Pricing" is a variable cost, that could eventually be part of the income, instead of the expenses, when the price for carbon rises further. Next to the variable costs, the fixed operational and maintenance costs are considered in Table 4.

Table 4: Annual Cost Breakdown

Cost Item	Cost [€/year]
Labour	352k
General and Administrative	1.76k
Property Taxes and Insurance	2,034k
Maintenance of Equipment	3,051k

For the personnel cost five plant operator with each working 1760 h/year at an hourly cost of 40 €/h have been considered. The general expenses are considered as 20% of the personnel cost [41]. The property taxes and insurance rate is taken as 2% of the investment costs [37], and the for the maintenance of the equipment 3% of the investment costs has been assumed [42]. Taxes are applied every year onto the income, decreased by depreciation and bank loan interests. The total tax rate in Belgium is 25% and for simplicity reason, no special tax benefits are assumed [43]. The proportions of OPEX costs are visualized in Figure 5 (right). An income generating stream next to the produced methanol is oxygen, which is a byproduct of the electrolysis and if sold generates an income of 3.4 mio € (see Table A.7 in appendix).

Economic Performance Indicator

The most interesting value for representing the profitability of the investment is the Levelized Cost of Methanol (LCoM). It gives the price at which the methanol must be sold to reach the break-even point at the end of the time span of the project. It tells the minimum price the product methanol needs to cover all expenses and is thereby a good indicator if the project is good to realize. The LCoM is calculated as follows:

The LCoM is calculated using equation 9.

$$\text{LCoM} = \frac{\sum_{t=0}^{T} \frac{(CC_t + OC_t) - (RO_t + E_t)}{(1+r)^t}}{\sum_{t=0}^{T} \frac{P_t}{(1+r)^t}} \tag{9}$$

where CC_t is the capital costs in year t (including initial investment and any subsequent replacement costs), OC_t is the total operating costs (including fixed cost, variable cost and cost in the senior debt refunding phase of 10 years) in year t, RO_t is the revenue from by-products (e.g., oxygen sales), E_t represents potential income through the negative CO_2 price, P_t is the annual methanol production in year t, r is the discount rate reflecting the time value of money and project risk, a rate of 7% is estimated for the project [44], T is the project lifetime (in years), and for t is the year ($t = 0$ during the construction period and $1 \leq t \leq 20$ during operation).

Carbon Pricing

For the emission of CO_2, the price is determined by the ETS (Emission Trading System). Since the investigated process is not generating emissions of CO_2 but consuming them, the CO_2 price in the ETS could be considered as a revenue, as it was performed by Sollai et al. [36]. The prices for 2024 are listed in [45]. An increase in carbon prices of 129 €/tCO_2 in 2030 and 212 €/tCO_2 in 2040 is assumed [46]. The prices for the period from 2025 to 2035 are calculated by linear interpolation, as displayed in Figure A.1. The costs for CO_2 supply are assumed to be 253.6 from flue gas amine wash €/tCO_2 [39].

5 Discussion

The LCoM value achieved is 1517,47 €/t as displayed in Table A.5 - A.10. This is more than twice the market price of methanol (700 €/t in January 2025 [47]). This result confirms that the production with assumed parameters is not yet cost-competitive compared to conventionally produced methanol. However, several economic and production factors used in the calculation can lead to improvements in the final price. A huge uncertainty is the assumed cost for CO_2. As described in chapter 4.2 it is likely that the cost for using CO_2 will decrease while the price for the Emission Trade System is increasing – possibly leading to a positive cash flow. Further importance lies on the chosen operational hours of the methanol plant and the electrolysis. This is due to the dynamic operation of the plant, dependent on the electricity cost. It is likely that the further expansion of renewable energies leads to temporarily very low energy prices which will lead to low average prices per MWh.

As displayed in Figure 5 a hydrogen buffer tank makes up almost a quarter of the total investment costs for the entire plant. Its size could be decreased by enabling partial load of the methanol plant [21, 20, 22] and choosing the load as a optimization variable with the goal of reducing plant downtime and/or tank size. The further expansion of hydrogen networks, as is discussed by F. Neumann [48] enables the usage of such a network as a buffer. Last, the assumed discount rate, interest rate of loan, or the share of equity, all have a significant influence on the LCoM and thereby the economic feasibility of the project.

Assuming optimistic conditions (H_2-tank replaced by H_2 network; average electricity cost for electrolysis of 10 €/MWh; CO_2 balance of ETS and carbon capture costs results in 200 €/t incoming cash flow) a LCoM of 600 €/t is resulting.

The calculations were also done with pure H_2 and CO_2. While this assumptions is reasonable for H_2 from electrolysis, CO_2 will likely contain impurities, which might interfere with reaction and separation.

6 Conclusion

In this work, a methanol production plant in a dynamic operation with the use of CO_2 and renewable energy was developed. The economic analysis showed that the process is not yet economically feasible but the work identified potential process improvements such as H_2 recovery with a membrane, energy integration with closed-cycle heat pumps in distillation, decoupling of electrolysis and methanol production as well as heat recovery. The highest share of energy in the synthesis process is consumed in the column, which could be decreased from 1.8 MW down to less than 0.4 MW. However, the energy demand of the process itself is a small proportion compared to the energy demand for electrolysis. With that in mind, it seems reasonable to put further effort on measures which reduce the cost for elecrolysis, such as optimized partial-load operation or H_2-recycling using membranes. Supportive policies and advancing technology could make green methanol a competitive alternative and contribute to a low-carbon future.

Code Availability

The code of the project is available at: https://github.com/MaikSa2/EURECHA_challenge

References

[1] George A Olah, Alain Goeppert, and GK Surya Prakash. *Beyond oil and gas: the methanol economy*. John Wiley & Sons, 2018.

[2] European Energy. European energy, 2025. URL https://europeanenergy.com/2025/03/12/european-energy-produces-first-raw-e-methanol-at-kasso/. [Accessed: 08.04.2025].

[3] Air Liquide. Air liquide, 2022. URL https://www.airliquide.com/group/press-releases-news/2022-12-12/air-liquide-fluxys-belgium-and-port-antwerp-bruges-awarded-eu-funding-building-antwerpc-co2-export. [Accessed: 11.02.2025].

[4] portofantwerp. methanol bunkering, 2024. URL https://newsroom.portofantwerpbruges.com/first-methanol-bunkering-with-deepsea-vessel-ane-maersk-at-port-of-antwerp-bruges. [Accessed: 11.02.2025].

[5] Éverton Simões Van-Dal and Chakib Bouallou. Design and simulation of a methanol production plant from co2 hydrogenation. *Journal of Cleaner Production*, 57:38–45, 2013. doi: furl10.1016/j.jclepro.2013.06.008.

[6] Sebastian Drünert, Ulf Neuling, Sebastian Timmerberg, and Martin Kaltschmitt. Power-to-x (ptx) from "excess electricity" in germany—economic analysis. *Zeitschrift für Energiewirtschaft*, 43:173–191, 2019.

[7] QuestOne. Pem-elektrolyseur me450, 2025. URL https://www.questone.com/produkte/detail/questone-pem-elektrolyseur-me450/me450/. [Accessed: 03.02.2025].

[8] Jeffrey R. Bartels, Michael B. Pate, and Norman K. Olson. An economic survey of hydrogen production from conventional and alternative energy sources. *International Journal of Hydrogen Energy*, 35(16):8371–8384, 2010. doi: 10.1016/j.ijhydene.2010.04.035.

[9] Jona Göbelbecker. Was kostet wasserstoff jetzt und in zukunft? *Chemie Technik*, 2022. URL https://www.chemietechnik.de/energie-utilities/wasserstoff/was-kostet-wasserstoff-jetzt-und-in-zukunft-338.html.

[10] Anton A. Kiss, J.J. Pragt, H.J. Vos, G. Bargeman, and M.T. de Groot. Novel efficient process for methanol synthesis by co2 hydrogenation. *Chemical Engineering Journal*, 284:260–269, 2016. doi: 10.1016/j.cej.2015.08.101.

[11] Gavin Towler. *Chemical engineering design : principles, practice, and economics of plant and process design*. Butterworth-Heinemann, an imprint of Elsevier, Kidlington, Oxford, Cambridge, MA, third edition edition, 2022. doi: 10.1016/C2019-0-02025-0.

[12] P Beeskow K. Herrera Delgado S. Pitter N. Dahmen J. Sauer B. Lacerda de Oliveira Campos, K. John. A detailed process and techno-economic analysis of methanol synthesis from h2 and co2 with intermediate condensation steps. *Processes*, 10(8), 2022.

[13] Dionysios S Karousos, Danial Qadir, Andreas A Sapalidis, Faizan Ahmad, and Evangelos P Favvas. Polymeric, metallic and carbon membranes for hydrogen separation: A review. *Gas Science and Engineering*, 2023.

[14] Norazlianie Sazali, Mohamad Azuwa Mohamed, and Wan Norharyati Wan Salleh. Membranes for hydrogen separation: A significant review. *The International Journal of Advanced Manufacturing Technology*, 107 (3):1859–1881, 2020.

[15] S. Datta Prasad C. Chakraborty S. Roy S. Singh Amarthaluri S. Dinda S. Kanuri, J. Vinodkumar Deeptank. Methanol synthesis from co2 via hydrogenation route: Thermodynamics and process development with techno-economic feasibility analysis. *Korean Journal of Chemical Engineering*, 40(4):810–823, 2023.

[16] David T Coker, BD Freeman, and GK Fleming. Modeling multicomponent gas separation using hollow-fiber membrane contactors. *AIChE journal*, 44(6):1289–1302, 1998.

[17] Quang Huy Pham, Eirini Goudeli, and Colin A Scholes. Selective separation of water and methanol from hydrogen and carbon dioxide at elevated temperature through polyimide and polyimidazole based membranes. *Journal of Membrane Science*, 686, 2023.

[18] Energy Charts. Electricity production and spot prices in belgium, 2025. URL https://energy-charts.info/charts/price_spot_market/chart.htm?l=en&c=BE&stacking=stacked_absolute_area&legendItems=010001. [Accessed: 22.02.2025].

[19] AL Klingler et al. Wasserstoffspeicher für dezentrale energiesysteme. *Fraunhofer-Institut für Arbeitswirtschaft und Organisation*, 2024.

[20] Chao Chen and Aidong Yang. Power-to-methanol: The role of process flexibility in the integration of variable renewable energy into chemical production. *Energy Conversion and Management*, 228:113673, 2021. doi: 10.1016/j.enconman.2020.113673.

[21] Xiaoti Cui, Søren Knudsen Kær, and Mads Pagh Nielsen. Energy analysis and surrogate modeling for the green methanol production under dynamic operating conditions. *Fuel*, 307:121924, 2022. doi: 10.1016/j.fuel.2021.121924.

[22] Viet Hung Nguyen, Arto Laari, and Tuomas Koiranen. The effect of green hydrogen feed rate variations on e-methanol synthesis by dynamic simulation. *Chemical Engineering Research and Design*, 212:293–306, 2024. doi: 10.1016/j.cherd.2024.11.012.

[23] Uri Ash-Kurlander, Oliver Martin, Luca D Fontana, Vikas R Patil, Men Bernegger, Cecilia Mondelli, Javier Pérez-Ramírez, and Aldo Steinfeld. Impact of daily startup–shutdown conditions on the production of solar methanol over a commercial cu–zno–al2o3 catalyst. *Energy Technology*, 4(5):565–572, 2016.

[24] Xin Gao, Xinshan Kong, Lixia Kang, and Yongzhong Liu. Analysis of dynamic characteristics of reconfigurable modular reactor systems for renewable methanol synthesis. *Industrial & Engineering Chemistry Research*, 63(43):18479–18496, 2024.

[25] Steffi Matthischke, Stefan Roensch, and Robert Güttel. Start-up time and load range for the methanation of carbon dioxide in a fixed-bed recycle reactor. *Industrial & Engineering Chemistry Research*, 57(18): 6391–6400, 2018. doi: 10.1021/acs.iecr.8b00755.

[26] Mirko Skiborowski. Fast screening of energy and cost efficient intensified distillation processes. *Chemical Engineering Transactions*, 69, 2018. doi: 10.3303/CET1869034.

[27] J. Bausa, R. v. Watzdorf, and W. Marquardt. Shortcut methods for nonideal multicomponent distillation: I. simple columns. *AIChE Journal*, 44(10):2181–2198, 1998. doi: 10.1002/aic.690441008.

[28] P. Giménez-Prades, J. Navarro-Esbrí, C. Arpagaus, A. Fernández-Moreno, and A. Mota-Babiloni. Novel molecules as working fluids for refrigeration, heat pump and organic rankine cycle systems. *Renewable and Sustainable Energy Reviews*, 167:112549, 2022. doi: 10.1016/j.rser.2022.112549.

[29] DM Van de Bor, CA Infante Ferreira, and Anton A Kiss. Low grade waste heat recovery using heat pumps and power cycles. *Energy*, 89:864–873, 2015.

[30] Z. Geng D. Wei, C. Liu. Conversion of low-grade heat from multiple streams in methanol to olefin (mto) process based on organic rankine cycle (orc). *Applied Sciences*, 10(10), 2020.

[31] Savvas L. Douvartzides, Aristidis Tsiolikas, Nikolaos D. Charisiou, Manolis Souliotis, Vayos Karayannis, and Nikolaos N. Taousanidis. Energy and exergy-based screening of various refrigerants, hydrocarbons and

siloxanes for the optimization of biomass boiler–organic rankine cycle (bb–orc) heat and power cogeneration plants. *Energies*, 15(15), 2022. ISSN 1996-1073. doi: 10.3390/en15155513.

[32] Munich Business School. Capex - bwl lexikon, 2025. URL https://www.munich-business-school.de/l/bwl-lexikon/capex. [Accessed: 20.01.2025].

[33] R. Sinnott G. Towler. Chapter 7 - capital cost estimating. In *Chemical Engineering Design (Second Edition)*, pages 307–354. Butterworth-Heinemann, Boston, second edition edition, 2013. doi: 10.1016/B978-0-08-096659-5.00007-9.

[34] Charlex Maxwell. Cost indices, 2024. URL https://toweringskills.com/financial-analysis/cost-indices/. [Accessed: 14.01.2025].

[35] Calmedia. Der währungsrechner, 2025. URL https://der-waehrungsrechner.de/USD/EUR. [Accessed: 22.02.2025].

[36] Stefano Sollai, Andrea Porcu, Vittorio Tola, Francesca Ferrara, and Alberto Pettinau. Renewable methanol production from green hydrogen and captured co2: A techno-economic assessment. *Journal of CO2 Utilization*, 68, 2023.

[37] Energy.Gov. Hydrogen program, 2025. URL https://www.hydrogen.energy.gov/program-areas/systems-analysis/h2a-analysis/h2a-production/h2a-prod-rules. [Accessed: 18.02.2025].

[38] A. Nicita, G. Maggio, A.P.F. Andaloro, and G. Squadrito. Green hydrogen as feedstock: Financial analysis of a photovoltaic-powered electrolysis plant. *International Journal of Hydrogen Energy*, 45(20):11395–11408, 2020. doi: 10.1016/j.ijhydene.2020.02.062.

[39] D. Leeson, N. Mac Dowell, N. Shah, C. Petit, and P.S. Fennell. A techno-economic analysis and systematic review of carbon capture and storage (ccs) applied to the iron and steel, cement, oil refining and pulp and paper industries, as well as other high purity sources. *International Journal of Greenhouse Gas Control*, 61:71–84, 2017. doi: 10.1016/j.ijggc.2017.03.020.

[40] A. Dutta J. Hensley L. J. Snowden-Swan D. Humbird J. Schaidle M. Biddy E. CD Tan, M. Talmadge. Conceptual process design and economics for the production of high-octane gasoline blendstock via indirect liquefaction of biomass through methanol/dimethyl ether intermediates. *Biofuels, Bioproducts and Biorefining*, 10(1):17–35, 2016.

[41] Szabolcs Szima and Calin-Cristian Cormos. Improving methanol synthesis from carbon-free h2 and captured co2: A techno-economic and environmental evaluation. *Journal of CO2 Utilization*, 24:555–563, 2018. doi: 10.1016/j.jcou.2018.02.007.

[42] Patrizio Battaglia, Giulio Buffo, Domenico Ferrero, Massimo Santarelli, and Andrea Lanzini. Methanol synthesis through co2 capture and hydrogenation: Thermal integration, energy performance and techno-economic assessment. *Journal of CO2 Utilization*, 44:101407, 2021. doi: 10.1016/j.jcou.2020.101407.

[43] pwv. Belgium corporate - taxes on corporate income, 2025. URL https://taxsummaries.pwc.com/belgium/corporate/taxes-on-corporate-income?utm_source. [Accessed: 18.02.2025].

[44] A. Azadeh, S.F. Ghaderi, M. Anvari, and M. Saberi. Performance assessment of electric power generations using an adaptive neural network algorithm. *Energy Policy*, 35(6):3155–3166, 2007. doi: 10.1016/j.enpol.2006.11.012.

[45] SENDECO2. Co2 prices of previous years, 2025. URL https://www.sendeco2.com/it/prezzi-co2. [Accessed: 11.02.2025].

[46] Robert C. Pietzcker, Sebastian Osorio, and Renato Rodrigues. Tightening eu ets targets in line with the european green deal: Impacts on the decarbonization of the eu power sector. *Applied Energy*, 293:116914, 2021. doi: 10.1016/j.apenergy.2021.116914.

[47] Methanex. Durchschnittlicher preis für methanol auf dem europäischen markt in den jahren von 2012 bis 2025. *Chemie Technik*, 2025. URL https://de.statista.com/statistik/daten/studie/730823/umfrage/durchschnittlicher-preis-fuer-methanol-auf-dem-europaeischen-markt/.

[48] M. Victoria T. Brown F. Neumann, E. Zeyen. The potential role of a hydrogen network in europe. *Joule*, 7(8):1793–1817, 2023.

[49] T. Nyberg M. Hernández Leal O. Lysenko M. Karlsson L. Karlsson L. Önnby E. Östling E. Lindblad M. Elevant K. Lundkvist M. Gustavsson, M. Särnbratt. Potential use and market of oxygen as a by-product from hydrogen production, 2023. URL https://energiforsk.se/media/32358/potential-use-and-market-of-oxygen-as-a-by-product-from-hydrogen-production-energiforskrapport-2023-937.pdf. [Accessed: 10.04.2025].

Appendix

Tables

Table A.1: Comparison of processes with and without membrane

Comparison Terms	**Process without Membrane**	**Process with Membrane**
%CO_2 utilized	80.6	86.2
%H_2 utilized	75.9	98.6
%H_2 loss	24	1.4
%CO_2 loss	19.4	13.8
%Carbon Yield of Methanol	95.6	88.5
CO produced (kmol/hr)	2.3	1

Table A.2: Values for correlation for estimation of equipment cost

Equipment	**Unit for Size, S**	**a**	**b**	**n**
Reactor	Volume [m^3]	61,500	32,500	0.8
Pressure Vessels	Shell Mass [kg]	250,000	17,400	0.85
Packing	[m^3]	0	7,600	1.0
Trays	Diameter [m]	130	440	1.8
Exchanger	Area [m^2]	28,000	54	1.2
Evaporator	Area [m^2]	330	36,000	0.55
Compressor	Power [kW]	260,000	2,700	0.75
Pump	Power [kW]	-1,100	2,100	0.6
Filter	Area [m^2]	-73,000	93,000	0.3

Table A.3: Typical Factors for Estimation of Project Fixed Capital Cost

Item	**Definition**	**Value [-]**
f_p	Installation factor for piping	0.8
f_{er}	Installation factor for equipment erection	0.3
f_{el}	Installation factor for electrical work	0.2
f_i	Installation factor for instrumentation and process control	0.3
f_c	Installation factor for civil engineering work	0.3
f_s	Installation factor for structures and buildings	0.2
f_l	Installation factor for lagging, insulation, or paint	0.1
f_m (Stainless Steel)	Materials Cost Factors Relative to Plain Carbon Steel	1.3

Table A.4: Updated Investment Costs of Equipment

Equipment	**Investment (2010) [€]**	**Investment Basis [€]**	**Investment Actual [€]**
Reactor	407,954	1,173,652	1,702,093
Rectification Column	1,502,684	4,323,107	6,269,604
Flash	319,228	774,494	1,331,907
Heat Exchangers	326,499	939,313	1,362,243
Membrane	287,194	826,234	1,198,249
Compressor	1,839,072	5,290,870	7,673,106
Turbine	680,552	1,957,897	2,839,449
Pumps	29,340	50,120	72,686

Table A.5: General Cost Overview

Cost Category	**Unit Cost**	**Units/Info**	**Quantity/Usage**
Operation hours electrolysis	-	h/yr.	2342
Operation hours methanol plant	-	h/yr.	5571
Total Overnight Costs (TOC)	-	€	101,686,715
Energy cost electrolysis	0.02178	€/kWh	-
Energy cost methanol plant	0.04489	€/kWh	-

Table A.6: Fixed and Variable Operating Costs

Category	**Unit Cost**	**Unit**	**Quantity**	**Total Cost (€/yr)**
Fixed Operating Costs				
Personnel Cost [41]	40 €	per hour	8,800 hours	352,000
G&A [41]	0.2	*100%	-	1,760
Property Tax & Insurance [37]	0.02	*100% of TOC	-	2,033,734
Maintenance [42]	0.03	*100% of TOC	-	3,050,601
Variable Operating Costs				
Power Cons. Electrolysis [18]	-	kWh/year	234,200,000	5,100,876
Power Cons. Methanol Plant [18]	-	kWh/year	15,208,830	682,724
Power Cons. (Start/Shut)	-	kWh/year	1,343,160	60,294
Water Cost [38]	0.01 €	per kg H_2O	18,400 kg/h	430,928
Catalyst Cost [40]	18.1 €	per kg	135 kg	2,444

Table A.7: Investment and Financing Costs

Investment Component	**Total Cost (€)**
Tank	25,033,378
Electrolyzer	54,204,000
Methanol Plant	22,449,337
CO2 Pricing	
ETS (Emission Trading System)	170 €/t
CO2 Capture	-250 €/t

Table A.8: Revenues from H_2, O_2, Methanol, and CO_2 Costs

Output	**Price (€/kg)**	**Quantity (kg/h)**	**Total Revenue (€)**
H_2	-	1840	-
O_2 [49]	0.1	14,720	3,447,424
Methanol (Jan 2025 price) [47]	0.7	3,202.89	12,490,310
CO_2 Cost [39] (used in methanol synthesis)	-0.08	5,149.15	-2,294,873

Table A.9: Assumptions and Yearly Rate Calculation

Assumptions	**Value**	**Unit**
Discount Factor (r)	0.07	*100%
Interest Rate of Loan (i)	0.06	*100%
Financing Loan Amount (K)	0.75	*100% of total capital cost
Senior Debt Refunding Period (n)	10.00	years
Plant Operating Lifetime	1.33	%
Depreciation Time Rest of Plant	10.00	years
Plant Construction Time	1.00	year
Yearly Rate Calculation	$A = \frac{(K \times i)}{1-(1+i)^{-n}}$	
Resulting Yearly Rate	10,430,813.20	€

Table A.10: LCoM Calculation

Year	**Discount Factor**	**CC**	**OC + RO - E**	**P**
1	0.93	101,686,715.04	121,306,924.81	16,675.98
2	0.87	0.00	18,336,644.64	15,585.03
3	0.82	0.00	17,137,051.07	14,565.45
4	0.76	0.00	16,015,935.58	13,612.57
5	0.71	0.00	14,968,164.09	12,722.03
...	...	...	...	...
20	0.26	0.00	2,729,631.15	4,611.05
Total	-	-	286,850,954.98	189,032.18
LCoM				**1,517.47 €/t**

Table A.11: Effect of split ratio on CO_2 utilization and H_2 loss

Split Ratio	**mol% CO_2 Utilized**	**mol% H_2 Loss**
0.50	38.00	6.81
0.40	38.65	5.28
0.15	40.62	15.25

Figures

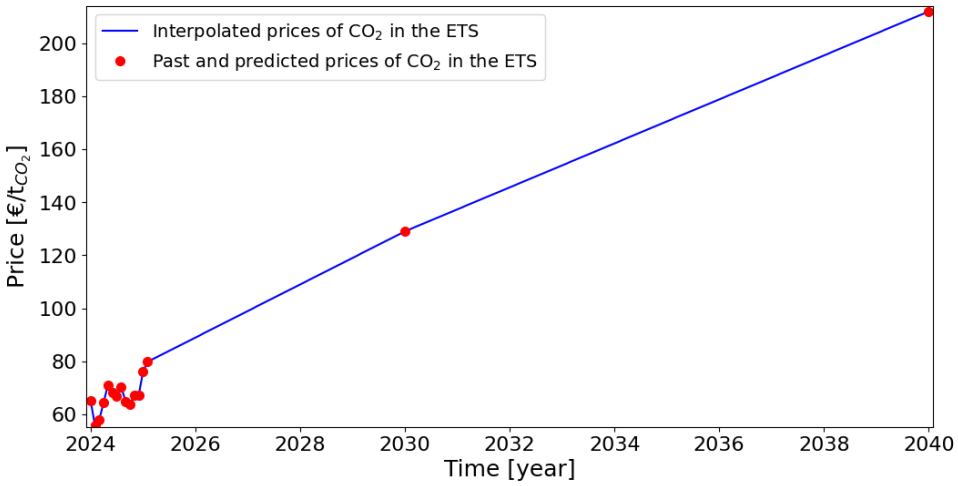

Figure A.1: Interpolation of carbon prices from 2024 to 2040 [45, 46].

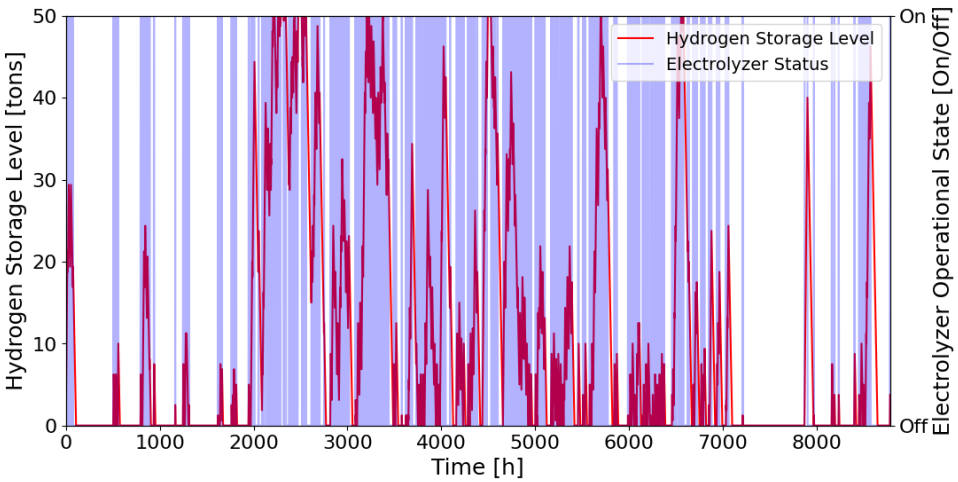

Figure A.2: Hydrogen accumulation and operation mode at a marginal price of 40 €/MWh

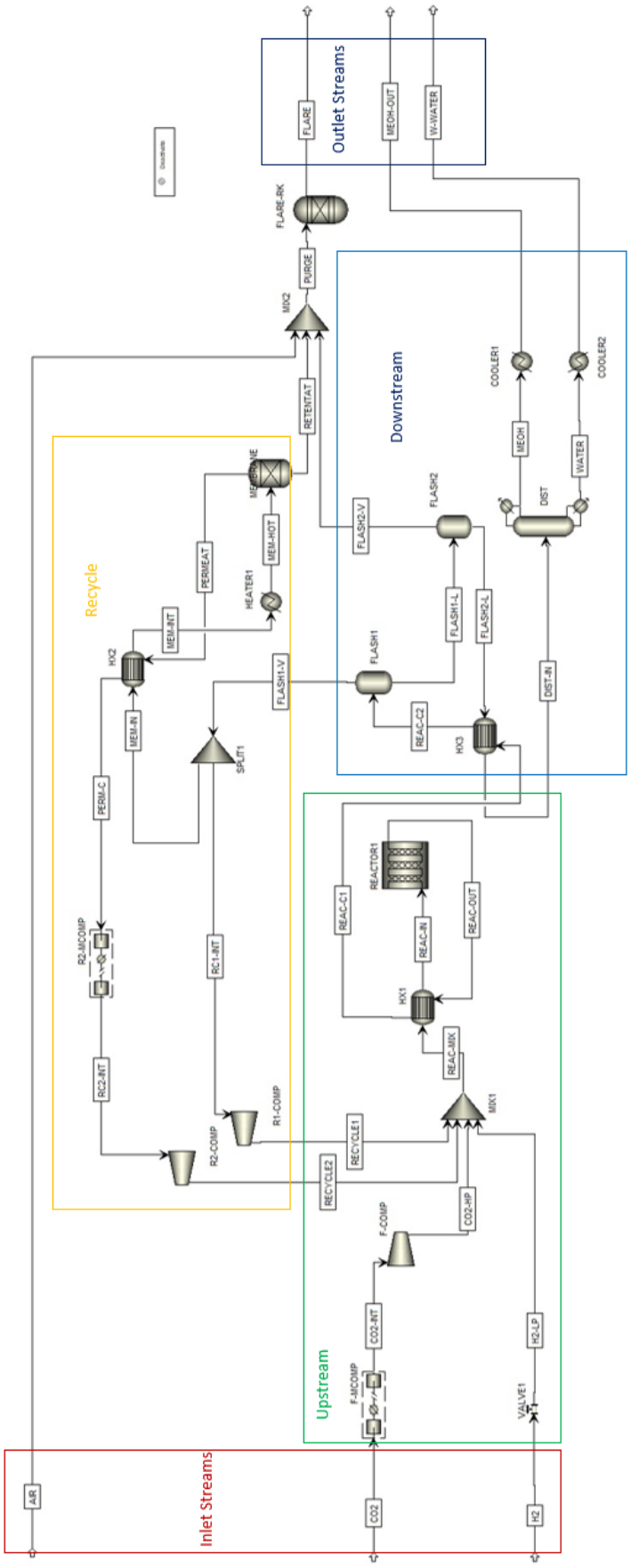

Figure A.3: Methanol synthesis Aspen Plus flowsheet

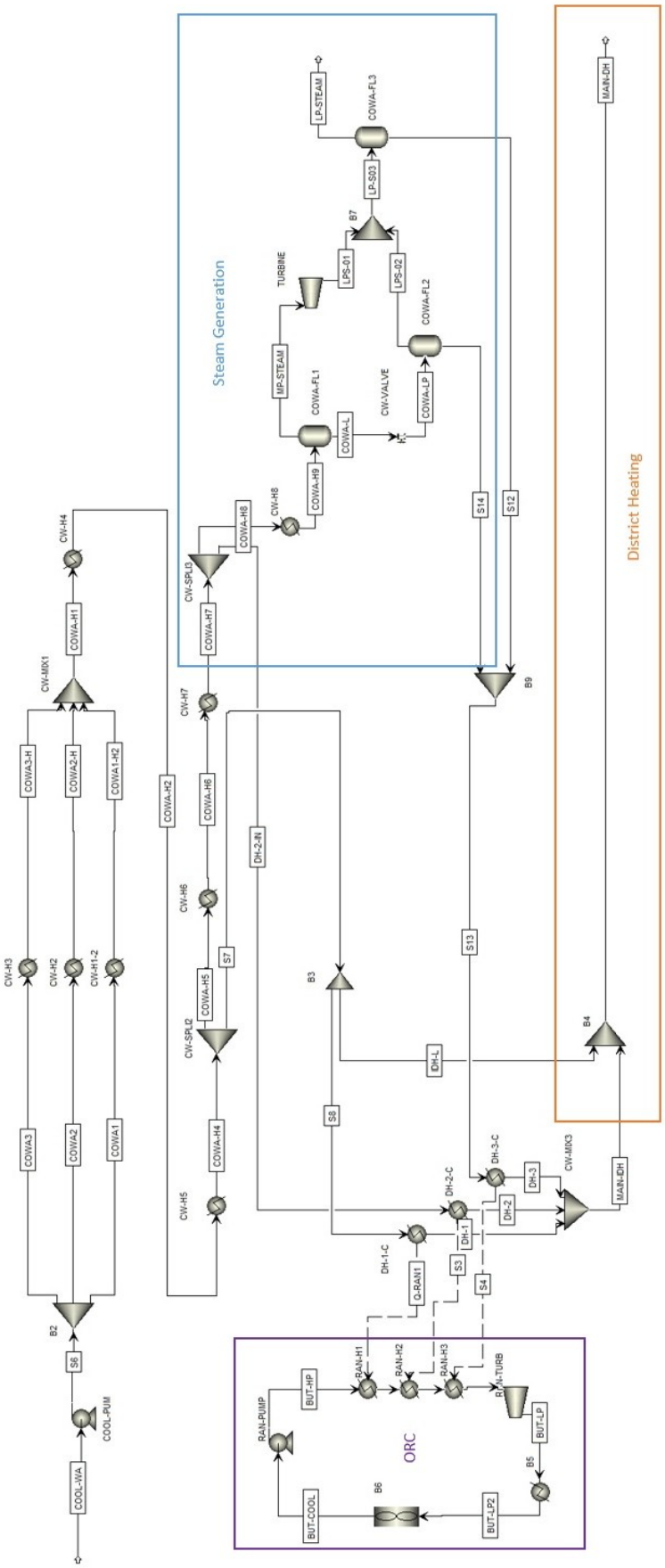

Figure A.4: Waste heat recovery Aspen Plus flowsheet

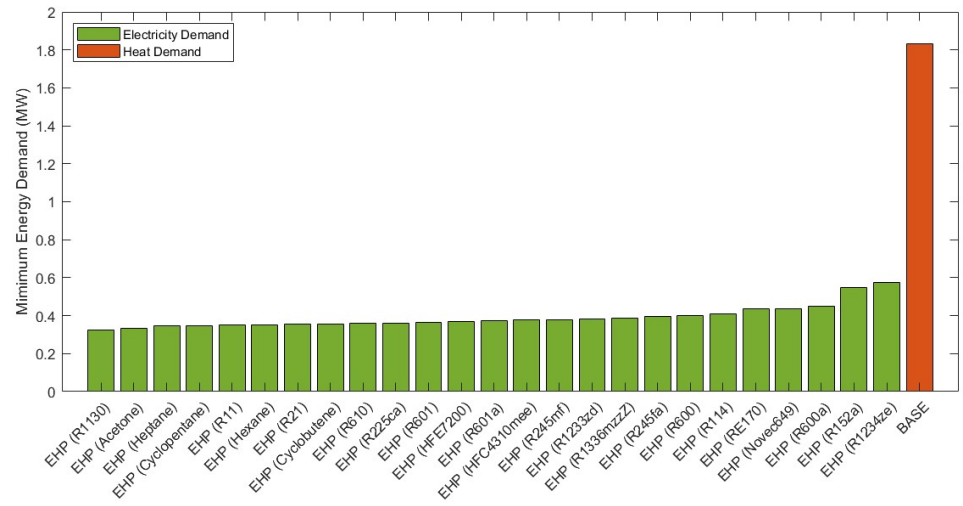

Figure A.5: Minimum energy demand of all calculated energy integrated columns

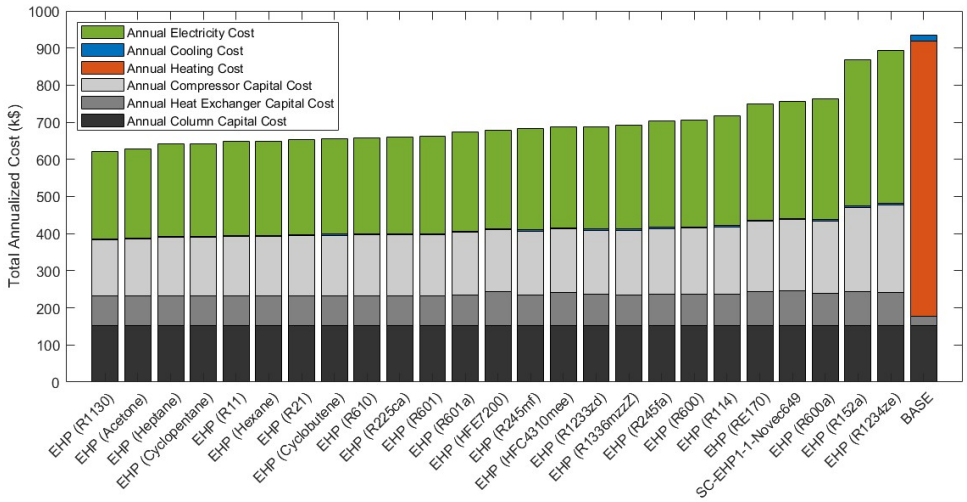

Figure A.6: Annualized total costs of all calculated energy integrated columns